

After 20 Years, Theoretical Evidence That “AuF₇” Is Actually AuF₅·F₂[†]Daniel Himmel[‡] and Sebastian Riedel^{*,§}*Institut für Anorganische und Analytische Chemie, Albert-Ludwigs Universität Freiburg, Albertstrasse 21, D-79104 Freiburg i. Br., Germany, and Department of Chemistry, University of Helsinki, A.I. Virtasen aukio 1, FIN-00014 Helsinki, Finland*

Received March 6, 2007

Quantum-chemical calculations at the DFT (BP86, PBE, TPSS, B3LYP, PBE0), MP2, CCSD, and CCSD(T) levels have been carried out to characterize the putative AuF₇ reported in 1986 by Timakov et al. Our calculations indicate clearly that the species claimed to be AuF₇ had not been synthesized. Instead, a new gold fluoride complex AuF₅·F₂ was prepared. This complex is 205 kJ mol⁻¹ more stable than the proposed AuF₇ species, and the elimination of F₂ is calculated to be endothermic. This is consistent with the reported stability of the product. A reported experimental vibrational frequency at 734 cm⁻¹ was verified computationally to be the F–F stretching mode of the end-on coordinated F₂ molecule. This result is in line with the recently published trends in the highest attainable oxidation states of the 5d transition metals where Au(V) remains the highest oxidation state of gold.

Introduction

Twenty years ago a Russian group claimed the preparation of AuF₇.¹ Gold heptafluoride was synthesized as the product of the reaction of AuF₅ and atomic fluorine, when the latter was produced by an electric discharge in gaseous F₂. The product was instantly frozen at -196 °C and described as a yellow crystalline material, which rapidly decomposed above 100 °C. The initial product was characterized by gas-phase IR spectroscopy and showed a band at 734 ± 3 cm⁻¹ that was unusual for a gold fluoride, and elemental analysis did support “AuF₇”.

Recently, we have shown by quantum-chemical calculations that this experimental report of AuF₇ was highly improbable.² Our investigations have shown that concerted F₂ elimination from AuF₇ would be strongly exothermic by -145.2 kJ mol⁻¹ at the CCSD(T) level and that the corresponding barrier lies only 10 kJ mol⁻¹ above the *D*_{5h} minimum. The second decomposition channel, homolytic bond breaking, also shows a decomposition that is exothermic by -84.5 kJ mol⁻¹ at the CCSD(T) level. Furthermore, it was not possible, by use of quantum-chemical calculations, to confirm the experimental IR band at 734 ± 3 cm⁻¹. Our

calculated vibrational frequencies were always well below the experimental one. The highest calculated Au–F stretching frequencies of AuF₇ are 634, 592, and 589 cm⁻¹ at the B3LYP level. Until now, the nature of the species that had been synthesized under the aforementioned electrical discharge conditions was unknown and our prior investigations and had only shown that AuF₇ was unlikely to exist.²

In the present study, we identify the real product of the mentioned experiment and report a new class of gold fluorine compounds. State-of-the-art quantum-chemical calculations have been used to describe the structures, stabilities, transition states, and frequencies of the AuF₅·F₂ complex.

Computational Details

Molecular structures were optimized using density-functional theory (BP86,^{3,4} PBE,⁵ TPSS,^{6,7} B3LYP,^{8–11} PBE0^{12,13}), with the Gaussian03⁸ and Turbomole 5.8¹⁴ programs. Optimizations were followed by single-point energy calculations at the DFT, MP2, and high-level coupled-cluster (CCSD and CCSD(T)) levels. Quasirelativistic, energy-adjusted, small-core “Stuttgart-type” pseudopotentials (effective-core potentials, ECPs) were used for gold.¹⁵ The corresponding (8s6p5d)[7s3p4d] valence basis set for Au was

[†] Dedicated to Prof. Neil Bartlett on the occasion of his 75th birthday.^{*} To whom correspondence should be addressed. E-mail: sebastian.riedel@psichem.de. Fax: +358-9-191 50169.[‡] Albert-Ludwigs Universität Freiburg.[§] University of Helsinki.(1) Timakov, A. A.; Prusakov, V. N.; Drobyshevskii, Y. V. *Dokl. Akad. Nauk SSSR* **1986**, *291*, 125–128.(2) Riedel, S.; Kaupp, M. *Inorg. Chem.* **2006**, *45*, 1228–1234.(3) Becke, A. D. *Phys. Rev. A* **1988**, *38*, 3098–3100.(4) Perdew, J. P. *Phys. Rev. B* **1986**, *33*, 8822–8824.(5) Perdew, J. P.; Burke, K.; Ernzerhof, M. *Phys. Rev. Lett.* **1996**, *77*, 3865–3868.(6) Tao, J.; Perdew, J. P.; Staroverov, V. N.; Scuseria, G. E. *Phys. Rev. Lett.* **2003**, *91*, 146401–146405.(7) Perdew, J. P.; Tao, J.; Staroverov, V. N.; Scuseria, G. E. *J. Chem. Phys.* **2004**, *120*, 6898–6911.

augmented by two f-type polarization functions (α_{f1} , Au 0.2 and α_{f2} , 1.19). The diffuse function, α_{f1} 0.2, maximizes the static polarizability, and the compact f-function, α_{f2} 1.19, improves the description of the primary covalent bonding to the metal.¹⁶ For comparison, we have also used the def2-TZVP basis set for Au,¹⁷ implemented in the Turbomole 5.8¹⁴ program, to optimize the AuF₅·F₂ complex (Table S1). In the optimizations, a fluorine DZ+P all-electron basis set by Dunning was used.¹⁸

Stationary points on the potential energy surface were characterized by harmonic vibrational frequency analyses at the DFT level (providing also zero-point energy corrections to the thermochemistry). Subsequent single-point energy calculations using the B3LYP optimized structures had the fluorine basis replaced by a larger aug-cc-pVTZ basis set.¹⁹ The post-HF calculations were carried out with the MOLPRO 2006.1 program package.²⁰ Basis-set superposition errors (BSSE) were not estimated. They were found to be small (5–10 kJ mol⁻¹) in previous studies.^{2,21–23}

Thus, all gold fluoride species calculated have singlet ground state configurations as shown in ref 2. In addition, the new AuF₅·F₂ complex is calculated to have a singlet ground state electronic configuration as the preferred minimum, i.e., the optimized triplet structure lies 34.7 kJ mol⁻¹ above the singlet one.

Note that the methodology used here, in particular the B3LYP optimizations followed by B3LYP or CCSD(T) single-point energy calculations with larger basis sets, is well established as a reliable tool for redox thermochemistry in the 5d transition metal series, e.g., previous studies of Hg,²¹ Au,² Pt,^{24,25} and Ir²² systems. Spin–

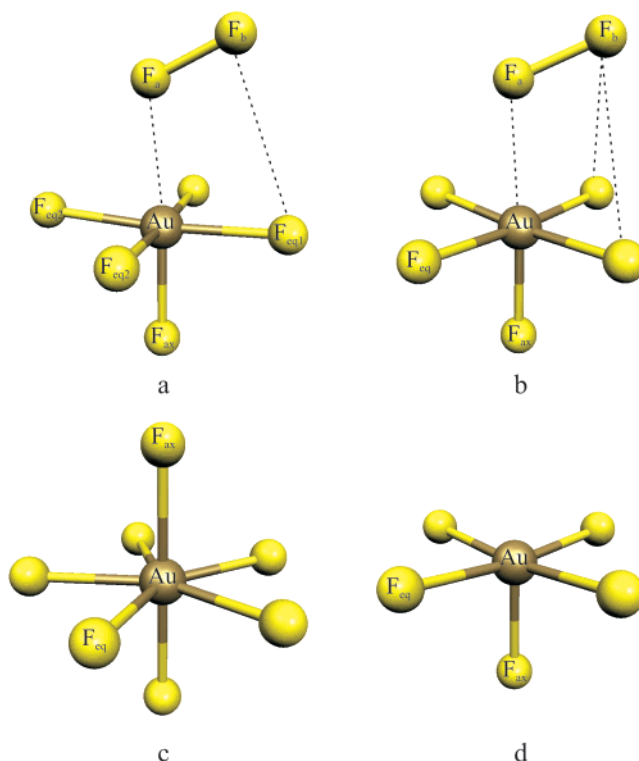


Figure 1. B3LYP-optimized structures (singlets) of gold fluoride complexes: (a) minimum structure of AuF₅·F₂ (C_s), (b) transition state of AuF₅·F₂ (C_s), (c) minimum structure of AuF₇ (D_{5h}), and (d) minimum structure of AuF₅ (C_{4v}).

orbit corrections are not considered in this work. Our previous studies indicated that spin–orbit effects have only a minor influence on the relevant thermochemical data and activation barriers, even when open-shell 5d species were involved.²²

Results and Discussion

The singlet AuF₅·F₂ complex can be described as a monomeric AuF₅ molecule showing a distorted square pyramidal structure with an end-on coordinated F₂ molecule in the axial position (C_s symmetry, Figure 1a, Table 1). The structural influence of the coordinated F₂ molecule on the C_{4v} symmetry of the AuF₅ moiety is marginal (Figure 1). The equatorial fluorine atoms are slightly longer in the AuF₅·F₂ complex and the axial fluorine bond distance is slightly shortened when compared with the AuF₅ structure. This may be due to the F₂ coordination in the axial position because the NPA charge of the axial fluorine atom (F_{ax}) of the complex is larger when compared with that of the AuF₅ moiety (Table 2). Furthermore, the NPA charges show a charge separation for the coordinated F₂ molecule where the positive charge is located on the F_b atom (Figure 1).

The F₂ bond distance of 140.5 pm in the complex is almost equal to that of the free F₂ molecule, 140.1 pm (experimental 141.7 pm).²⁶ This is also the case for the second AuF₅·F₂ complex where the F₂ molecule is coordinated between the two equatorial fluorine atoms, forming a dihedral angle

- (8) Frisch, M. J.; Trucks, G. W.; Schlegel, H. B.; Scuseria, G. E.; Robb, M. A.; Cheeseman, J. R.; Montgomery, J. A., Jr.; Vreven, T.; Kudin, K. N.; Burant, J. C.; Millam, J. M.; Iyengar, S. S.; Tomasi, J.; Barone, V.; Mennucci, B.; Cossi, M.; Scalmani, G.; Rega, N.; Petersson, G. A.; Nakatsuji, H.; Hada, M.; Ehara, M.; Toyota, K.; Fukuda, R.; Hasegawa, J.; Ishida, M.; Nakajima, T.; Honda, Y.; Kitao, O.; Nakai, H.; Klene, M.; Li, X.; Knox, J. E.; Hratchian, H. P.; Cross, J. B.; Bakken, V.; Adamo, C.; Jaramillo, J.; Gomperts, R.; Stratmann, R. E.; Yazyev, O.; Austin, A. J.; Cammi, R.; Pomelli, C.; Ochterski, J. W.; Ayala, P. Y.; Morokuma, K.; Voth, G. A.; Salvador, P.; Dannenberg, J. J.; Zakrzewski, V. G.; Dapprich, S.; Daniels, A. D.; Strain, M. C.; Farkas, O.; Malick, D. K.; Rabuck, A. D.; Raghavachari, K.; Foresman, J. B.; Ortiz, J. V.; Cui, Q.; Baboul, A. G.; Clifford, S.; Cioslowski, J.; Stefanov, B. B.; Liu, G.; Liashenko, A.; Piskorz, P.; Komaromi, I.; Martin, R. L.; Fox, D. J.; Keith, T.; Al-Laham, M. A.; Peng, C. Y.; Nanayakkara, A.; Challacombe, M.; Gill, P. M. W.; Johnson, B.; Chen, W.; Wong, M. W.; Gonzalez, C.; Pople, J. A. *Gaussian 03*, revision B.04; Gaussian, Inc.: Pittsburgh, PA, 2003.
- (9) Becke, A. D. *J. Chem. Phys.* **1993**, *98*, 5648–5652.
- (10) Lee, C.; Yang, W.; Parr, R. G. *Phys. Rev. B* **1988**, *37*, 785–789.
- (11) Miehlich, B.; Savin, A.; Stoll, H.; Preuss, H. *Chem. Phys. Lett.* **1989**, *157*, 200–206.
- (12) Adamo, C.; Barone, V. *J. Chem. Phys.* **1999**, *110*, 6158–6170.
- (13) Ernzerhof, M.; Scuseria, G. E. *J. Chem. Phys.* **1999**, *110*, 5029–5036.
- (14) Ahlrichs, R.; Bär, M.; Häser, M.; Horn, H.; Kölmel, C. *Chem. Phys. Lett.* **1989**, *162*, 165–169.
- (15) Andrae, D.; Häussermann, U.; Dolg, M.; Stoll, H.; Preuss, H. *Theor. Chim. Acta* **1990**, *77*, 123–141.
- (16) Pyykkö, P. *Angew. Chem., Int. Ed.* **2004**, *43*, 4412–4456.
- (17) Weigend, F.; Ahlrichs, R. *Phys. Chem. Chem. Phys.* **2005**, *7*, 3297–3305.
- (18) Dunning, T. H., Jr. *J. Chem. Phys.* **1970**, *53*, 2823–2833.
- (19) Dunning, T. H., Jr. *J. Chem. Phys.* **1989**, *90*, 1007–1023.
- (20) Werner, H.-J.; Knowles, P. J.; Lindh, R.; Manby, F. R.; Schütz, M.; Celani, P.; Korona, T.; Rauhut, G.; Amos, R. D.; Bernhardsson, A.; Berning, A.; Cooper, D. L.; Deegan, M. J. O.; Dobbyn, A. J.; Eckert, F.; Hampel, C.; Hetzer, G.; Lloyd, A. W.; McNicholas, S. J.; Meyer, W.; Mura, M. E.; Nicklass, A.; Palmieri, P.; Pitzer, R.; Schumann, U.; Stoll, H.; Stone, A. J.; Tarroni, R.; Thorsteinsson, T. *MOLPRO 2006.1*; a package of ab initio programs; University College Cardiff Consultants Limited: Birmingham, U.K., 2006.
- (21) Riedel, S.; Straka, M.; Kaupp, M. *Phys. Chem. Chem. Phys.* **2004**, *6*, 1122–1127.
- (22) Riedel, S.; Kaupp, M. *Angew. Chem., Int. Ed.* **2006**, *45*, 3708–3711.
- (23) Riedel, S.; Kaupp, M. *Inorg. Chem.* **2006**, *45*, 10497–10502.

- (24) Wesendrup, R.; Schwerdtfeger, P. *Inorg. Chem.* **2001**, *40*, 3351–3354.
- (25) Riedel, S. *J. Fluorine Chem.* DOI:10.1016/j.jfluchem.2007.04.001.
- (26) Weast, R. C., Ed. *CRC Handbook of Chemistry and Physics*. 68th ed.; CRC Press: Boca Raton, FL, 1987.

Table 1. Optimized Molecular Structures (Singlet Minima) of Gold Fluorides ($\text{AuF}_5 \cdot \text{F}_2$) with Bond Distances in pm and Angles in deg

	MP2	BP86	PBE	TPSS	PBE0	B3LYP	B3LYP ^a	$\text{AuF}_7 (D_{5h})$	B3LYP	$\text{AuF}_5 (C_{4v})$	B3LYP
$\text{F}-\text{F}^b$	142.3	141.9	141.7	141.9	138.2	140.1		$\text{Au}-\text{F}_{\text{ax}}$	193.3	$\text{Au}-\text{F}_{\text{ax}}$	188.0
F_a-F_b	142.7	145.3	145.2	144.9	138.4	140.5	140.5	$\text{Au}-\text{F}_{\text{eq}}$	194.7	$\text{Au}-\text{F}_{\text{eq}}$	192.0
F_a-Au	221.6	222.0	222.3	220.5	223.2	227.0				$\text{F}_{\text{ax}}-\text{Au}-\text{F}_{\text{eq}}$	93.8
$\text{Au}-\text{F}_{\text{ax}}$	188.6	189.8	189.7	189.0	185.3	187.4	187.3			$\text{F}_{\text{eq}}-\text{Au}-\text{F}_{\text{eq}}$	89.7
$\text{Au}-\text{F}_{\text{eq}1}$	193.4	193.6	193.6	193.0	190.5	192.4	192.4				
$\text{Au}-\text{F}_{\text{eq}2}$	193.4	194.4	194.3	193.7	190.6	192.5	192.4				
$\text{Au}-\text{F}_{\text{eq}3}$	193.6	195.7	195.8	194.8	190.5	192.6	192.4				
$\text{F}_b-\text{F}_a-\text{Au}$	107.0	118.5	118.3	118.1	113.5	113.5	112.6				
$\text{F}_{\text{eq}1}-\text{Au}-\text{F}_{\text{eq}3}$	176.9	172.2	172.0	172.5	175.4	175.0	175.4				
$\text{F}_{\text{eq}2}-\text{Au}-\text{F}_{\text{eq}2}$	176.9	175.5	175.5	175.7	176.0	175.8	175.4				
$\text{F}_{\text{ax}}-\text{Au}-\text{F}_b$	177.2	170.2	170.2	170.7	175.9	175.8	177.3				
$\text{F}_{\text{eq}1}-\text{Au}-\text{F}_{\text{eq}2}$	90.1	90.0	90.0	90.0	90.0	90.0	89.7				
$\text{F}_{\text{ax}}-\text{Au}-\text{F}_a-\text{F}_b$	45.3	0.0	0.0	0.0	1.2	0.2	44.9				

^a B3LYP-optimized transition state. ^b For comparison, the optimized bond distances of the free F_2 molecule. Experimental bond distance is 141.193 pm.²⁸

Table 2. Computed NPA Charges for $\text{AuF}_5 \cdot \text{F}_2$ and AuF_5

NPA	$\text{AuF}_5 \cdot \text{F}_2$	NPA	AuF_5
Au	2.221	Au	2.245
F_{ax}	-0.317	F_{ax}	-0.281
$\text{F}_{\text{eq}1}$	-0.501	F_{eq}	-0.491
$\text{F}_{\text{eq}2}$	-0.505	F_{eq}	-0.491
$\text{F}_{\text{eq}3}$	-0.505	F_{eq}	-0.491
F_a	0.017		
F_b	0.095		

Table 3. Optimized Transition-State Structures for Rotation of the End-On Coordinated F_2 Molecule for $\text{AuF}_5 \cdot \text{F}_2$

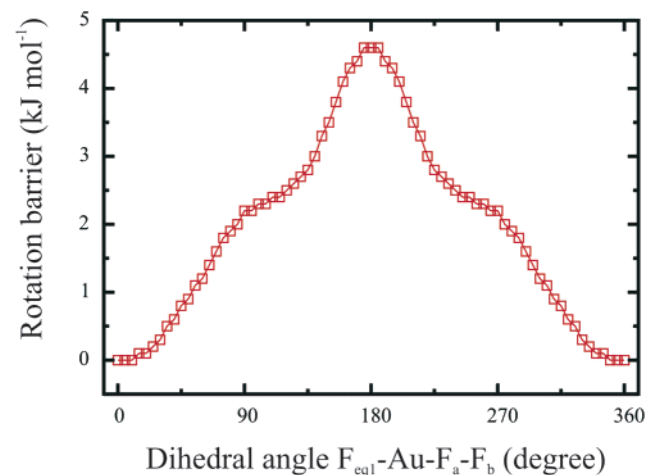
	B3LYP	MP2
Bond Distances (pm)		
F_a-F_b	140.5	140.5
F_a-Au	227.5	227.3
$\text{Au}-\text{F}_{\text{ax}}$	187.3	187.4
$\text{Au}-\text{F}_{\text{eq}1}$	192.4	192.3
$\text{Au}-\text{F}_{\text{eq}2}$	192.4	192.4
$\text{Au}-\text{F}_{\text{eq}3}$	192.4	192.6
Bond Angles (deg)		
$\text{F}_b-\text{F}_a-\text{Au}$	112.6	113.6
$\text{F}_{\text{eq}1}-\text{Au}-\text{F}_{\text{eq}3}$	175.4	174.9
$\text{F}_{\text{eq}2}-\text{Au}-\text{F}_{\text{eq}2}$	175.4	175.8
$\text{F}_{\text{ax}}-\text{Au}-\text{F}_b$	177.3	175.8
$\text{F}_{\text{eq}1}-\text{Au}-\text{F}_{\text{eq}2}$	89.7	89.9
$\text{F}_{\text{ax}}-\text{Au}-\text{F}_a-\text{F}_b$	45.0	0.0

($\text{F}_{\text{eq}}-\text{Au}-\text{F}_a-\text{F}_b$) of 45° (C_s symmetry, Figure 1b). This $\text{AuF}_5 \cdot \text{F}_2$ complex is calculated at the B3LYP level to be a transition state that is only 0.2 kJ mol^{-1} above the complex (Figure 1a), showing one imaginary frequency at $i11 \text{ cm}^{-1}$ (Table 3). This vanishingly small barrier, together with the very low imaginary frequency, indicates a very shallow potential energy surface. Indeed, scanning the potential energy surface by rotating the F_2 molecule around the z -axis ($\text{F}_{\text{ax}}-\text{Au}-\text{F}_a$) while keeping the AuF_5 structure fixed gives a barrier of only 4.6 kJ mol^{-1} (Figure 2). Optimizations of both $\text{AuF}_5 \cdot \text{F}_2$ complexes at the MP2 level reverses the energetics. The complex shown in Figure 1a is a transition state at the MP2 level that is 3.5 kJ mol^{-1} above the calculated minimum for the complex shown in Figure 1b (Table 3). Again, these level dependencies indicate a shallow potential energy surface for the rotating F_2 molecule. Because of our prior positive experiences with the use of the B3LYP functional, for optimized structures and single-point calculations of the thermochemistry,^{2,21–23,25,27} they have again been

Table 4. Computed Single-Point Reaction Energies (in kJ mol^{-1})^a

reactions	B3LYP	ZPE ^b	MP2	CCSD	CCSD(T) ^c
$\text{AuF}_5 \cdot \text{F}_2 \rightarrow \text{AuF}_5 + \text{F}_2$	27.1	22.2	52.0	46.6	48.8
$\text{AuF}_7 \rightarrow \text{AuF}_5 + \text{F}_2$	-160.5	-166.5	-58.2	-235.7	-152.0
$\text{AuF}_5 \cdot \text{F}_2 \rightarrow [\text{AuF}_6]^- + \text{F}^+$	997.7	993.9	976.9	950.4	976.3

^a Reaction energies for (singlet) $\text{AuF}_5 \cdot \text{F}_2$ and AuF_7 . ^b Zero-point vibration corrected energies (B3LYP level) using the DZ+P basis set for fluorine. ^c T_1 -diagnostics: $\text{AuF}_5 \cdot \text{F}_2$ (0.020), AuF_7 (0.020), $[\text{AuF}_6]^-$ (0.021), AuF_5 (0.024).

**Figure 2.** Rotational barrier of the F_2 coordinated molecule in the $\text{AuF}_5 \cdot \text{F}_2$ complex at the B3LYP level. The AuF_5 unit was kept fixed by rotation around the $\text{F}_{\text{eq}1}-\text{Au}-\text{F}_a-\text{F}_b$ dihedral angle; the angle was incremental in 5° steps.

used in the ensuing discussion. Gold heptafluoride is $205.5 \text{ kJ mol}^{-1}$ higher in energy than the $\text{AuF}_5 \cdot \text{F}_2$ complex (Figure 1a). The enormous stability of the $\text{AuF}_5 \cdot \text{F}_2$ complex when compared with that of AuF_7 is the first strong indication that the former species was actually produced in the original experiment.¹

To establish the stability of the $\text{AuF}_5 \cdot \text{F}_2$ complex, we have calculated the concerted F_2 elimination energies of $\text{AuF}_5 \cdot \text{F}_2$ and AuF_7 . Our calculations show endothermic reaction paths for all computational levels used in this study up to and including CCSD(T) for the reaction $\text{AuF}_5 \cdot \text{F}_2 \rightarrow \text{AuF}_5 + \text{F}_2$ (Table 4). This contrasts with the F_2 -elimination energy of AuF_7 , where all calculated elimination energies were exo-

(27) Riedel, S.; Straka, M.; Kaupp, M. *Chem.—Eur. J.* **2005**, *11*, 2743–2755.

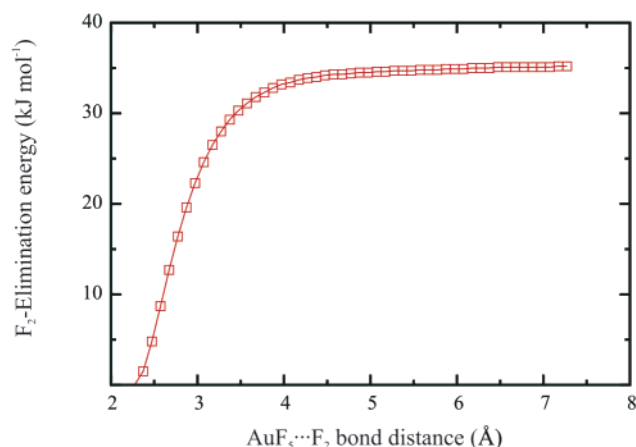


Figure 3. B3LYP-scan of the potential energy surface by stepwise elongation (10 pm per step) of the F₂–AuF₅ bond distance, starting from the AuF₅·F₂ minimum bond distance of 227.3 pm.

thermic (Table 4 and ref 2). Scanning the potential energy surface by stepwise elongation of the F₂–AuF₅ bond distance leads to a barrier of 35.2 kJ mol^{−1} at the B3LYP level (Figure 3). This endothermic F₂ elimination, together with the barrier, accounts for the explanation of the experimentally observed stability of the product (note that the stability will be generally somewhat more positive in the condensed phase as a result of electrostatic stabilization of the complexes) which was stable up to 100 °C in the gas phase and decomposed rapidly into AuF₅ and F₂ at higher temperatures.

As we have already reported,² the identification of the AuF₇ species was based, in particular, on vibrational spectroscopy. In our prior study, we calculated the spectra of all higher gold fluorides, i.e., AuF₅, AuF₆, AuF₇, [AuF₅]₂, [AuF₅]₃, and [AuF₆][−], but none of them showed a frequency higher than 647 cm^{−1} in the [AuF₅]₂ dimer. The latter frequency is appreciably lower than the experimental value of 734 ± 3 cm^{−1}.^{1,2} Instead, the AuF₅·F₂ complex has a calculated frequency at 1012 cm^{−1} at the B3LYP level. This frequency is slightly lower than that of the free F₂ molecule at 1052 cm^{−1} (B3LYP). However, the B3LYP functional overestimates the F–F stretching mode by 135 cm^{−1} when compared with the experimental value of 916.64 cm^{−1}.²⁸ This effect is known and is mainly due to the strongly interacting lone pairs of the F₂ molecule.^{29,30} As was shown by Scott and Radom,³¹ the vibrational frequencies of the F₂ molecule are difficult to describe at the DFT level and GGA functionals tend to give slightly better results than the hybrid ones. This is not only true for F₂ but has been verified in other studies of main-group compounds and transition-metal complexes that the GGA functionals better reproduce vibrational frequencies.^{32–35}

(28) Huber, K. P.; Herzberg, G. *Molecular Spectra and Molecular Structure, 4: Constants of Diatomic Molecules*; Van Nostrand Reinhold: New York, 1979.

(29) Koch, W.; Holthausen, M. C. *A Chemist's Guide to Density Functional Theory*, 2nd ed.; Wiley-VCH: Weinheim, Germany, 2001.

(30) Forslund, L. E.; Kaltsoyannis, N. *New J. Chem.* **2003**, *27*, 1108–1114.

(31) Scott, A. P.; Radom, L. *J. Phys. Chem.* **1996**, *100*, 16502–16513.

(32) Holthausen, M. C. *J. Comput. Chem.* **2005**, *26*, 1505–1518.

(33) Florian, J.; Johnson, B. G. *J. Phys. Chem.* **1994**, *98*, 3681–3687.

(34) Hertwig, R. H.; Koch, W. *J. Comput. Chem.* **1995**, *16*, 576–585.

Table 5. Harmonic Vibrational Frequency Analysis at DFT and MP2 Levels

MP2		BP86		PBE		TPSS		B3LYP		PBE0	
freq ^a	int ^b	freq ^a	int ^b	freq ^a	int ^b	freq ^a	int ^b	freq ^a	int ^b	freq ^a	int ^b
27	0	60	3	60	9	63	0	48	0	57	0
96	0	61	1	63	2	65	2	83	0	98	0
110	0	124	2	127	3	125	0	121	0	126	0
154	0	127	0	129	0	129	3	142	1	150	1
179	0	148	0	148	1	152	1	174	1	184	1
186	0	159	0	161	0	165	0	178	0	189	0
189	1	168	0	169	1	168	0	188	0	197	0
204	0	184	0	185	0	189	0	196	0	208	0
244	8	224	9	227	7	228	10	241	17	252	11
246	0	230	1	229	3	231	3	249	2	258	6
249	5	231	4	232	4	232	4	249	4	263	2
312	20	272	1	275	1	284	1	275	11	296	16
543	1	537	4	534	2	553	3	571	0	595	0
554	0	543	0	541	1	557	1	575	0	598	0
621	6	591	53	589	53	607	60	632	96	655	106
642	64	601	78	600	76	617	78	632	94	656	107
643	63	611	22	610	20	628	21	648	11	680	13
962 ^c	1	779 ^c	104	775 ^c	105	809 ^c	75	1010 ^c	1	1065 ^c	1
969 ^d		1001 ^d		1002 ^d		1012 ^d		1052 ^d		1101 ^d	
7 ^e		222 ^e		227 ^e		203 ^e		42 ^e		36 ^e	

^a Frequencies in cm^{−1}. ^b IR intensities in km mol^{−1}. ^c F–F stretching mode of the coordinated F₂ molecule in cm^{−1}. ^d F–F stretching mode of the free F₂ molecule in cm^{−1}. Experimental value is 916.64 cm^{−1}.²⁸ ^e Difference between the F–F stretching mode (Δfrequency) of the AuF₅·F₂ complex and the free F₂ molecule in cm^{−1}.

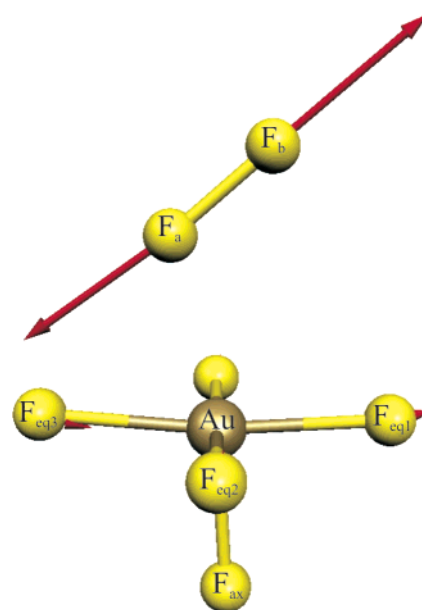


Figure 4. BP86-optimized minimum structure of the AuF₅·F₂ complex. The F–F stretching mode at 779 cm^{−1} is indicated by displacement vectors.

Because of these observations, we have also used several GGA functionals (BP86, PBE, and TPSS) to calculate the vibrational spectra of the AuF₅·F₂ complex (Table 5). Indeed, the BP86 and PBE functionals resulted in much lower frequencies when compared with the hybrid functionals (Table 5). The BP86 and PBE functionals give the stretching mode of the F₂ molecule at 779 and 775 cm^{−1}, respectively. We may therefore confidently assign the experimental band of 734 ± 3 cm^{−1} to be the F–F stretching mode in the AuF₅·F₂ complex (Figure 4).

(35) Jonas, V.; Thiel, W. *J. Chem. Phys.* **1995**, *102*, 8474–8484.

Conclusions

In summary, we have shown that all experimental observations of Timakov et al. done in 1986 can be right.¹ The $\text{AuF}_5 \cdot \text{F}_2$ complex fits well to the molecular weight determination because $\text{AuF}_5 \cdot \text{F}_2$ has the same stoichiometry as AuF_7 . The complex is calculated to be thermochemically stable and is far more stable than the AuF_7 minima. Scanning the potential energy surface leads to an activation barrier of 35.2 kJ mol⁻¹. Last but not least, the experimentally measured IR frequency at 734 ± 3 cm⁻¹ is in accord with the F–F stretching mode of the $\text{AuF}_5 \cdot \text{F}_2$ complex. We therefore conclude that the experimentally assigned product, AuF_7 , was in reality $\text{AuF}_5 \cdot \text{F}_2$. This complex would not only be a new gold complex but also be, up to the present, the first complex in which AuF_5 is a coordinating unit.^{16,36} Thus far, gold pentafluorides have only been observed as AuF_5 species or as hexafluoroaurate anions $[\text{AuF}_6]^-$ containing several other species.³⁷ The compound would also be the first example of difluorine acting as a Lewis-base in a condensed phase. Furthermore, the $\text{AuF}_5 \cdot \text{F}_2$ complex sup-

(36) Pyykkö, P. *Inorg. Chim. Acta* **2005**, 358, 4113–4130.

(37) Mohr, F. *Gold Bull. (Geneva)* **2004**, 37, 164–169.

ports our recently published trend of the highest attainable oxidation states of the 5d transition metals, where it is shown that the highest oxidation state that can be expected for gold is the +V oxidation state.^{22,23,25}

Because the $\text{AuF}_5 \cdot \text{F}_2$ complex is a stable crystalline solid, it should be possible to verify its structure by, for example, an X-ray crystal structure determination or by electron diffraction.

Acknowledgment. The authors are grateful to P. Pyykkö and D. Sundholm for stimulating discussions and to M. Kaupp and I. Krossing for kindly providing computational resources. S.R. thanks the Alexander von Humboldt Foundation for a Feodor Lynen Research Fellowship. D.H. thanks the DFG for a postdoctoral fellowship. This project belongs to the Finnish CoE in Computational Molecular Science.

Supporting Information Available: Optimized $\text{AuF}_5 \cdot \text{F}_2$ structures using the def2-TZVP basis set for Au (Table S1) and B3LYP-optimized structures of the triplet states of $\text{AuF}_5 \cdot \text{F}_2$ (Table S2). This material is available free of charge via the Internet at <http://pubs.acs.org>.

IC700431S